Electronic Supplementary Material (ESI) for CrystEngComm.

SUPPLEMENTARY/SUPPORTING INFORMATION

Recurrent motifs in pharmaceutical cocrystals involving Glycolic acid: X-ray characterization, Hirshfeld surface analysis and DFT calculations

C. Alvarez-Lorenzo,[a] A. Castiñeiras,*[b] A. Frontera,[c] I. García-Santos,[b] J. M. González-Pérez,[d] J. Niclós-Gutiérrez,[d] I. Rodríguez-González,[b] E. Vílchez-Rodríguez,[b] and J. K. Zaręba[e]

[a].*University of Santiago de Compostela, Department of Pharmacy and Pharmaceutical Technology, Faculty of Pharmacy, 15782 Santiago de Compostela, Spain.*

[b].*University of Santiago de Compostela, Department of Inorganic Chemistry, Faculty of Pharmacy, 15782 Santiago de Compostela, Spain.*

[c] *Departament de Química, Universitat de les Illes Balears, Crta. de Valldemossa km 7.5, 07122 Palma de Mallorca (Baleares), Spain.*

[d] *University of Granada, Department of Inorganic Chemistry, Faculty of Pharmacy, 18071 Granada, Spain.*

[e] *Advanced Materials Engineering and Modelling Group, Wrocław University of Science and Technology, Wyb. Wyspiańskiego 27, 50370, Wrocław, Poland.*

CONTENTS

CRYSTALLOGRAPHIC TABLES 3
PXRD PATTERN 5
FT-IR ANALYSIS. 6
POWDER X-RAY DIFFRACTION ANALYSIS. 8
THERMAL ANALYSIS. 9
DSC ANALYSIS. 11
HIRSHFELD SURFACE ANALYSIS 12
COMPARISON OF HS PROPERTIES OF 1 WITH THOSE OF PURE ACID (CSD REFCODE GLICAC01) 19
REFERENCES 20

Crystallographic tables

Table S1. Hydrogen bond parameters [Å, °] for the compounds studied

Compound	D–H···A	D–H	H···A	D···A	∠DHA	Symmetry transformations
$[NH_4]$[GA-H]·GA (**1**)	O(21)-H(21) ···O(11)[a]	0.92	1.61	2.531(1)	179.0	-x, y-1/2, -z+1/2
	O(23)-H(23)···O(12)	0.82	1.88	2.692(1)	168.7	
	O(13)-H(13)···O(12)[c]	0.83	1.91	2.733(1)	171.3	x, -y+1/2, z-1/2
	N(1)-H(1)···O(22)[e]	0.91	2.17	2.948(1)	142.7	-x+1, -y, -z
	N(1)-H(2)···O(13)[d]	0.91	2.02	2.923(1)	176.7	x+1, y, z
	N(1)-H(3)···O(23)	0.94	1.90	2.815(1)	165.3	
	N(1)-H(4)···O(11)[c]	0.92	1.95	2.864(1)	174.8	-x+1, -y, -z
(PA)/(GA) (**2**)	N(10)-H(10A)···O(12)[h]	0.91	2.14	2.933(2)	146(2)	-x+2, -y+1, -z
	N(10)-H(10B)···O(12)[r]	0.94	1.99	2.899(2)	162(2)	x-1, y, z-1
	O(11)-H(11A)···O(10)[k]	0.94	1.66	2.586(2)	171(2)	-x+1/2, y+1/2, -z+3/2
	O(13)-H(13A)···N(13)[h]	0.83	2.44	3.110(2)	139(3)	-x+2, -y+1, -z
	O(13)-H(13A)···O(12)	0.83	2.21	2.680(2)	116(2)	
2(NA)/(GA) (**3**)	N(10)-H(10A)···O(13)[a]	0.83	2.07	2.869 (1)	162.1	x+1/2, -y, z+1/2
	N(10)-H(10B)···O(20)[b]	0.89	2.06	2.943 (1)	174.0	-x+1/2, -y+1, z+1/2
	N(20)-H(20A)···O(10)[d]	0.87	2.00	2.869(1)	176.7	-x+1/2, -y+1, z-1/2
	N(20)-H(20B)···O(11)	0.85	2.18	2.989(1)	158.6	
	O(11)-H(11A)···N(24)[e]	0.97	1.63	2.598(1)	178.2	x, -y+1/2, z-1/2
	O(13)-H(13A)···N(14)[c]	0.92	1.81	2.732(1)	176.8	-x+1/2, y-1/2, z
(IN)/(GA) (**4**)	N(10)-H(10A)···O(10)[f]	0.90	2.03	2.926(1)	176.5	-x+1, -y+1, -z+1
	N(10)-H(10B)···O(12)[g]	0.90	2.07	2.976(1)	177.3	x+1, y, z
	O(11)-H(11)···N(15)[h]	0.93	1.68	2.612(1)	172.9	-x+2, -y+1
	O(13)-H(13A)···O(10)[f]	0.85	1.97	2.805(1)	169.5	-x+1, -y+1, -z+1
(CA)/2(GA) (**5**)	O(11)-H(11)···O(22)	0.91	1.76	2.665(2)	178.8	
	O(13)-H(13)···O(2)[u]	0.85	1.94	2.777(2)	168.2	-x, -y+1, -z+1
	O(21)-H(21)···N(9)[v]	1.03	1.59	2.614(2)	172.7	-x, -y+1, -z
	O(23)-H(23)···O(12)[w]	0.87	2.43	3.183(2)	146.1	x+1/2, y, -z+1/2
	O(23)-H(23)···O(13)[w]	0.87	2.14	2.877(2)	143.0	x+1/2, y, -z+1/2
(TP)/(FA) (**6**)	N(7)-H(7)···O(19)[h]	0.90	1.84	2.741(6)	175(5)	-x+2, -y+1, -z
	N(10)-H(10A)···O(6)[h]	0.99	1.88	2.872(6)	176(4)	-x+2, -y+1, -z
	N(10)-H(10B)···N(9)[r]	0.91	2.05	2.954(7)	175(5)	x-1, y, z-1

Table S2. Intermolecular interaction parameters (Å, °) for the compounds studied.

Compound	$\pi\cdots\pi$ *interactions*	Cg(I)···Cg(J)	α	Symmetry transformations
2(NA)/(GA) (**3**)	Cg(1)···Cg(2)	3.666	3.27	
	Cg(1)···Cg(2)[a]	3.641	2.64	1/2+x, y, 1/2-z
	Cg(2)···Cg(1)	3.666	3.27	
	Cg(2)···Cg(1)[b]	3.641	2.64	-1/2+ x, y, 1/2-z
Cg(1): ring (N14/C13/C12/C17/C16/C15); Cg(2): ring (N24/C23/C22/C27/C26/C25)				
(CA)/2(GA) (**5**)	Cg(1)···Cg(1)[a]	3.482	0.00	-x,-1/2+y, -z
	Cg(1)···Cg(1)[b]	3.482	0.00	-x, 1/2-y, -z
	Cg(1)···Cg(1)[c]	3.482	0.00	-x, -y, -z
	Cg(1)···Cg(1)[d]	3.482	0.00	-x, 1-y, -z
Cg(1): ring N7/C5/C4/N9/C8				
(TP)/(FA) (**6**)	Cg(1)···Cg(2)[a]	3.332	1.00	2-x, 1-y, -z
	Cg(2)···Cg(1)[a]	3.332	1.00	
	Cg(2)···Cg(2)[a]	3.822	0.00	
Cg(1): ring (N7/C5/C4/N9/C8); Cg(2): ring (N1/C2/N3/C4/C5/C6)				

Cg(I)···Cg(J): Distance between ring centroids; α: Dihedral angle between planes I and J.

PXRD pattern

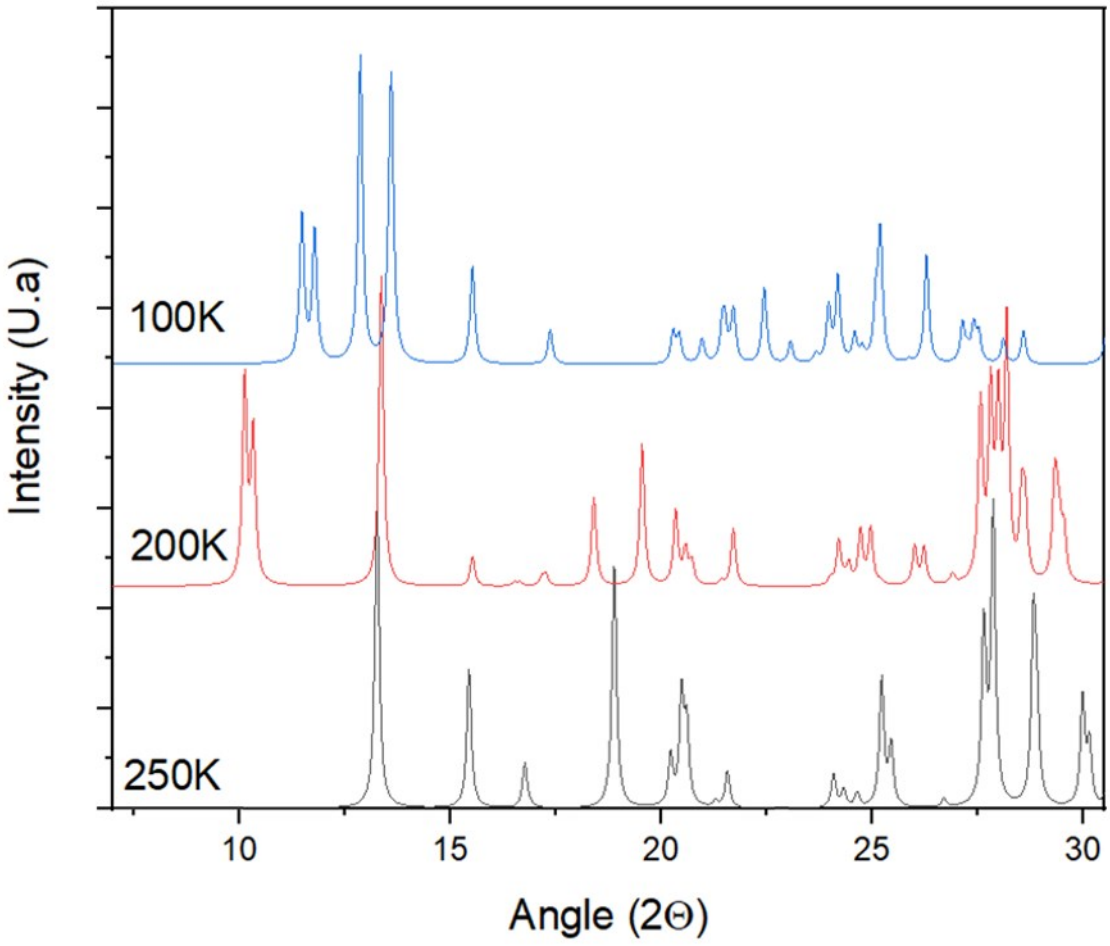

Figure S1. PXRD patterns of the three TP-FA solid forms obtained at 250 K (Form I), 200 K (Form II) and 100 K (Form III). The PXRD patterns of all the TP-FA products match well with the simulated PXRD patterns of RACDUX (CCDC-1440527), RACDUX01, (CCDC-1440528) and compound **6**.

FT-IR analysis.

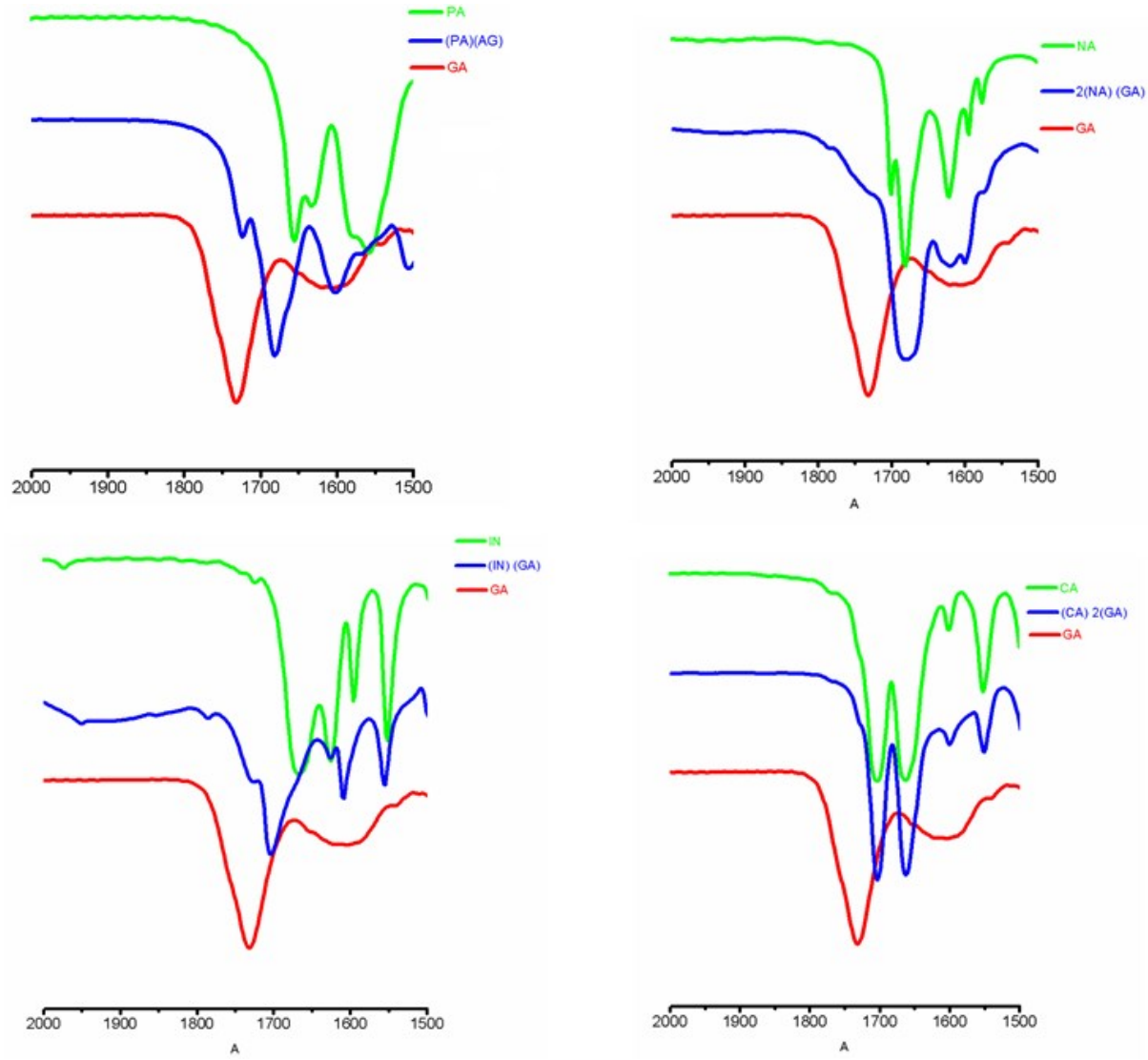

Figure S2. Fragment of FTIR spectra of glycolic (red trace), coformers (green trace), and their cocrystal compounds (a) (PA)/(GA) (**2**), (b) 2(NA)/(GA) (**3**), (c) (IN)/(GA) (**4**) and (d) (CA)/2(GA) (**5**).

IR spectroscopy is often a suitable technique to detect the formation of cocrystals, especially when carboxylic acids are used and/or when hydrogen bonds of type O-H···N are formed between both coformers.[1] In the region 3500-3000 cm^{-1} of the spectra appear the stretching vibrations v(OH) and v(NH), which wavenumber is very sensitive to the hydrogen bond formation.[2] The wide and intense band of glycolic acid close to 3500 cm^{-1} is due to the OH stretching modes of the hydroxyl group (3590-3400 cm^{-1}) and the carboxyl group (3300-2500 cm^{-1}), which are superimposed. Its position indicates the presence of intermolecular hydrogen bonding. In cocrystal structures this band appears about 3200 cm^{-1} because the hydrogen bond persists, now between the molecules of the coformers. On the other hand, the stretching vibrations v(NH) of the primary amide group of the

pyridinecarboxamides are manifested in two sharp bands of medium intensity due to the asymmetric and symmetrical modes that appear between 3350-3200 cm^{-1}. Both bands are maintained in the spectra of cocrystals 2(NA)/(GA) and (IN)/(GA), distinguishing now in that region a set of three bands, where the highest frequency is due to the ν(OH) modes. The CH_3 stretching vibration of caffeine is observed at 2975-2950 cm^{-1} (asymmetric) and between 2885-2865 cm^{-1} (symmetric). Such bands are practically unchanged in the spectrum of (CA)/2(GA).

In the range 1900-1300 cm^{-1} (Fig. S2) the stretching modes C=O and also the vibrations C=C and C=N of the heterocycles appear. A characteristic difference in the IR spectra of a salt and a cocrystal formed from a carboxylic acid, can be observed at the position of the bands corresponding to the stretching modes ν(CO). The cocrystals must present two bands, a strong one near 1700 cm^{-1} and a weak one near 1275 cm^{-1}. However, salts containing the carboxylate group usually have a single band corresponding to the modes ν(COO^-) around 1650 cm^{-1}.[3] In the glycolic acid spectrum a band at 1735 cm^{-1} is observed which is assigned to ν(CO) and another at 1361 cm^{-1} assigned to ν(C-O)+δ(C-OH).[4] In cocrystal structures the first band appears displaced at lower frequencies, probably due to the participation of the oxygen atom in the characteristic intermolecular hydrogen bond C-O···H, and the second at slightly higher frequencies, confirming that co-crystals have been obtained and no salts. In the spectra of cocrystals (PA)/(GA), 2(NA)/(GA) and (IN)/(GA) the band due to the stretching vibration C=O of the amide group at 1650 cm^{-1}, moves to higher frequencies as a result of the formation of primary amide-carboxylic acid heterosynthons. In the spectrum of the caffeine cocrystal two strong and sharp bands at 1703 and 1662 cm^{-1} have been assigned to the stretching modes ν(C=O).

For (TP)/(FA), changes in the C=O stretching frequency of both coformers suggest that carbonyl groups should be involved in hydrogen bonding in the solvate, as acceptors. In addition, the N-H stretching vibrations shift to blue due to changes in the hydrogen bond structure of the N-H bonds as donors.

Powder X-ray Diffraction Analysis.

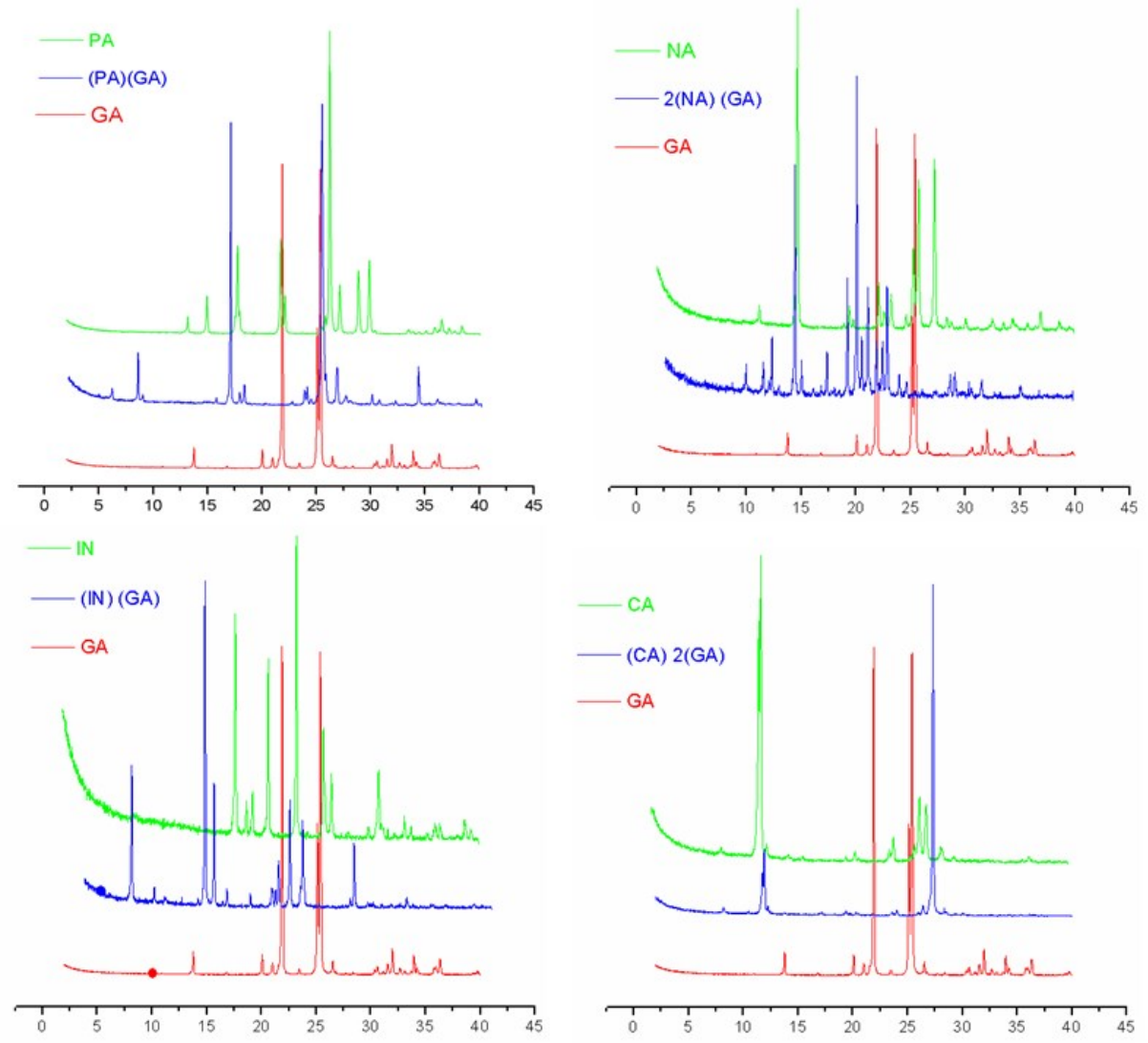

Figure S3. PXRD patterns of glycolic acid (red), coformers (green) and cocrystals (blue) in (a) (PA)/(GA) (**2**), (b) 2(NA)/(GA) (**3**), (c) (IN)/(GA) (**4**) and (d) (CA)/2(GA) (**5**).

As shown in Fig. S3, the PXRD patters of the 2(NA)·(GA, (IN)·(GA, and (CA)·2(GA) cocrystals were compared with those of coformers. The diffractogram from each cocrystal was clearly different from those of its pure constituents. In addition, a qualitative analysis of the obtained phases is carried out by comparing the diffractogram of each cocrystal with all the known polymorphs of the respective coformers reveals the phase purity of the cocrystals studied.

Thermal Analysis.

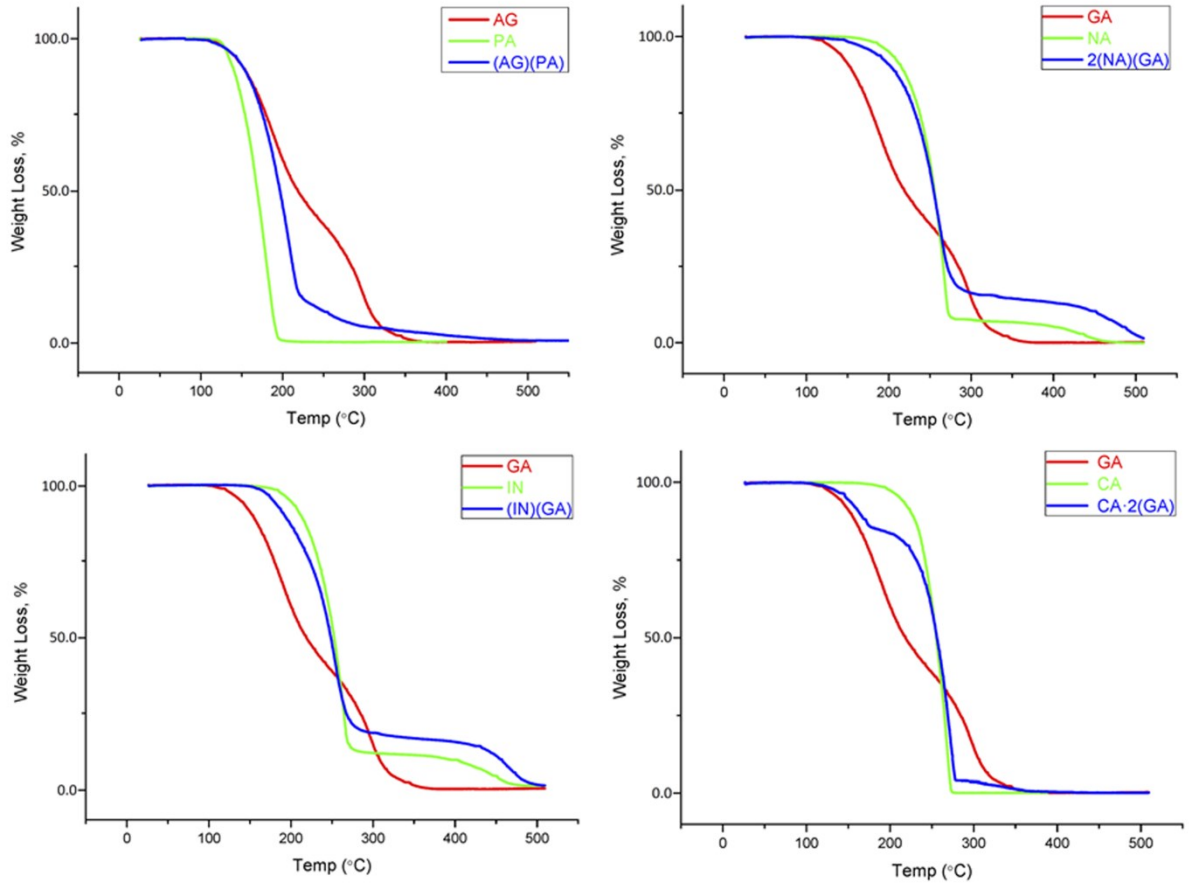

Figure S4. TG thermograms of pure components and the cocrystals **2**-**5**.

A thermogravimetric analysis was carried out to evaluate the stability of the cocrystals. Thermogravimetric records (Fig. S4) reveal that for (PA)/(GA) there is a weight loss of 96% of the sample between the ambient temperature and 320 °C. Most of this weight is lost between 100 and 220 °C, only the loss of CO_2, H_2O, H_2CO and traces of CO being recorded. This behavior suggests the sublimation of both PA (60% calc) and GA. At 380 °C, after two stages, the second small, the residue is approximately 2.3% that ends up decomposing at a higher temperature producing H_2O, CO_2, CO, N_2O and NO.

For 2(NA)/(GA), decomposition occurs in two global processes. In the first (75-315 °C) weight is lost (84.50%) in a much higher than expected proportion of the elimination of glycolic acid (38.38%), although the gases formed correspond to it (CO_2, H_2O, CO and H_2CO). In the second stage (315-565 °C) CO_2, H_2O and the nitrogen oxides (N_2O, NO and NO_2) observed in the second stage of pyrolytic decomposition of pure nicotinamide (240-420 °C) are released.

For cocrystal (IN)/(GA), in the first stage (120-310 °C) the gases inherent in the pyrolysis of glycolic acid appear to be released and also isonicotinamide sublimate (CO_2, H_2O, CO, H_2CO and N_2O). The

second one (370-550 °C) must correspond to the pyrolysis of isonicotinamide, not previously sublimated where CO_2, H_2O, CO and N_2O are released; not releasing ammonia. If we observed the habit of the first derivative, with the appearance of a saw in the first half of the first stage, we would see that sublimation is indicating us.

Finally, in the cocrystal (CA)/2(GA), the glycolic acid pyrolyze and caffeine sublimated with a partial decomposition that scarcely leaves trace of N_2O.

DSC analysis.

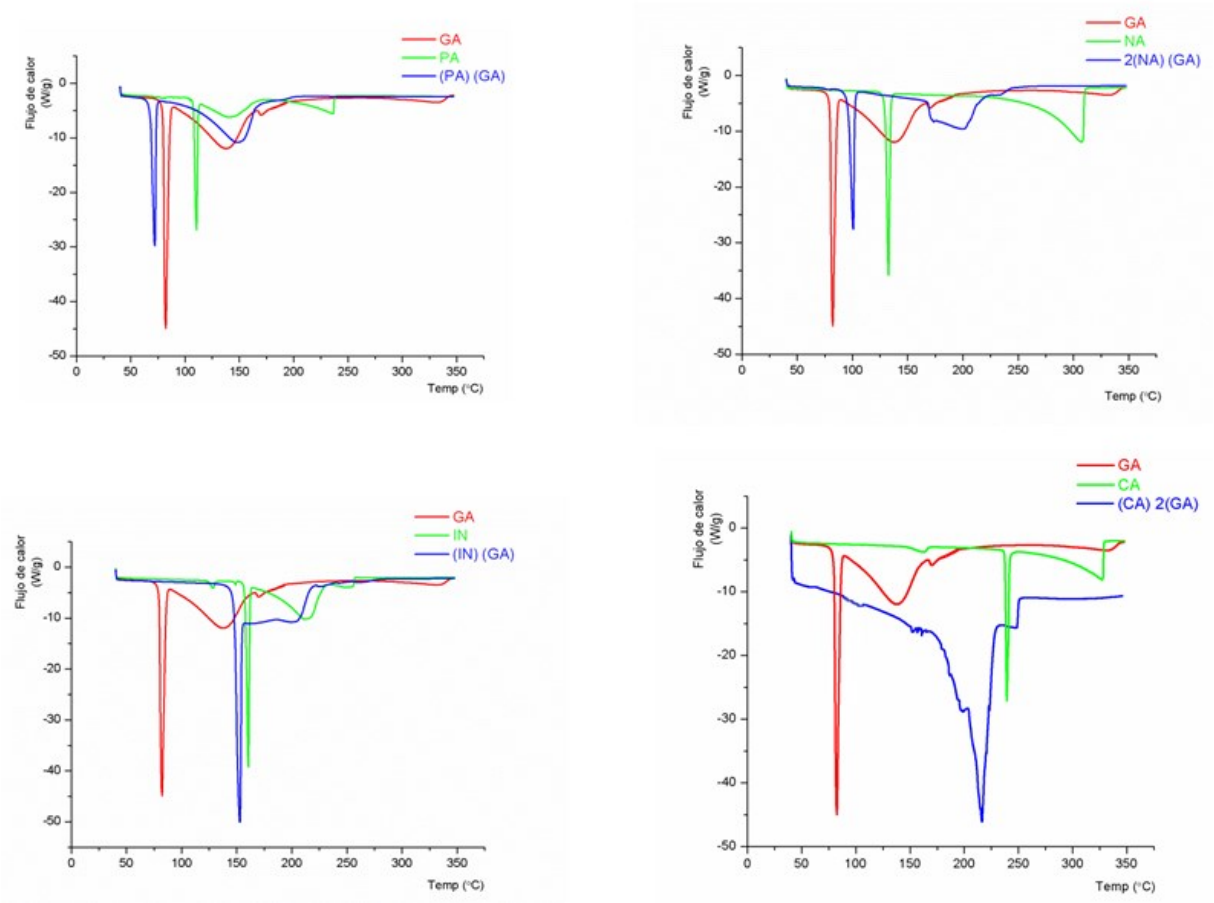

Figure S5. DSC analyses of the resulting powders of pure components and the cocrystals **2**-**5**.

Fig. S5 shows the heat flux versus the temperature for the glycolic acid, the coformers and the corresponding cocrystals. It can be observed that the melting points of the cocrystals are different from that of glycolic acid (82 °C) and those of the coformers PA (106 °C), NA (131 °C), IN (159 °C) and CA (238 °C). We find that for most cocrystals the melting point is between the melting points of the corresponding coformers. One exception is (PA)/(GA), for which it is below the melting points of glycolic acid and picolinamide.[5] This anomalous behavior might be due to its different hydrogen bonding behavior. Indeed, as we have demonstrated in the crystal structure description and Hirshfeld Surface analysis sections, PA molecule in **2** tends to form HB ring motifs with GA molecule, which leads to a smaller number of surrounding molecules (and therefore, smaller number of hydrogen bonds) with which hydrogen bonding occurs. This resulted in relative decrease of total share of strong HB contacts, and effected in the increase of percentage share of weak dispersion-related contacts (H···H). Accordingly, we take this observation from HS analysis as a tentative explanation why the melting point of **2** is suppressed, especially when compared to **3** and **4**.

Hirshfeld Surface analysis

N···H **O···H**

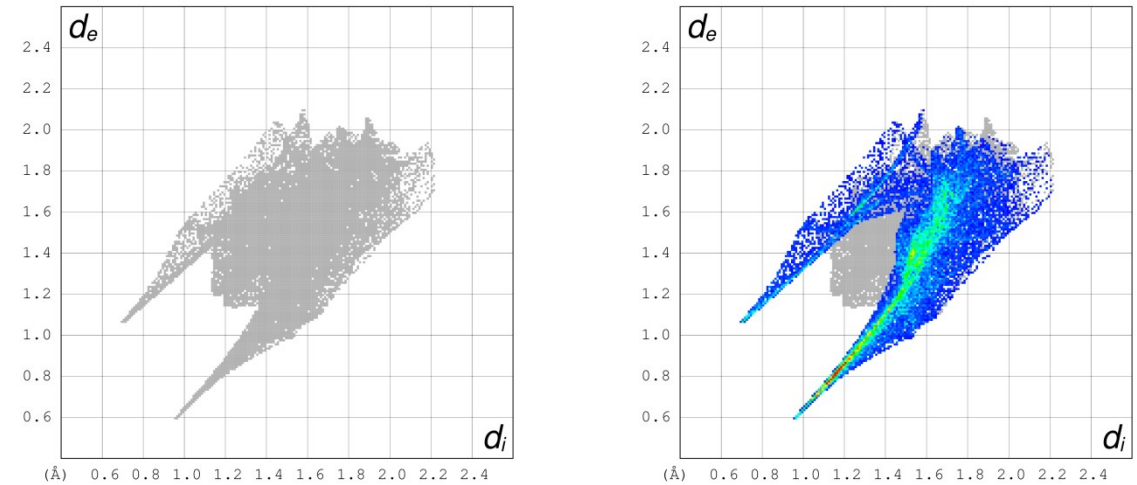

C···H **H···H**

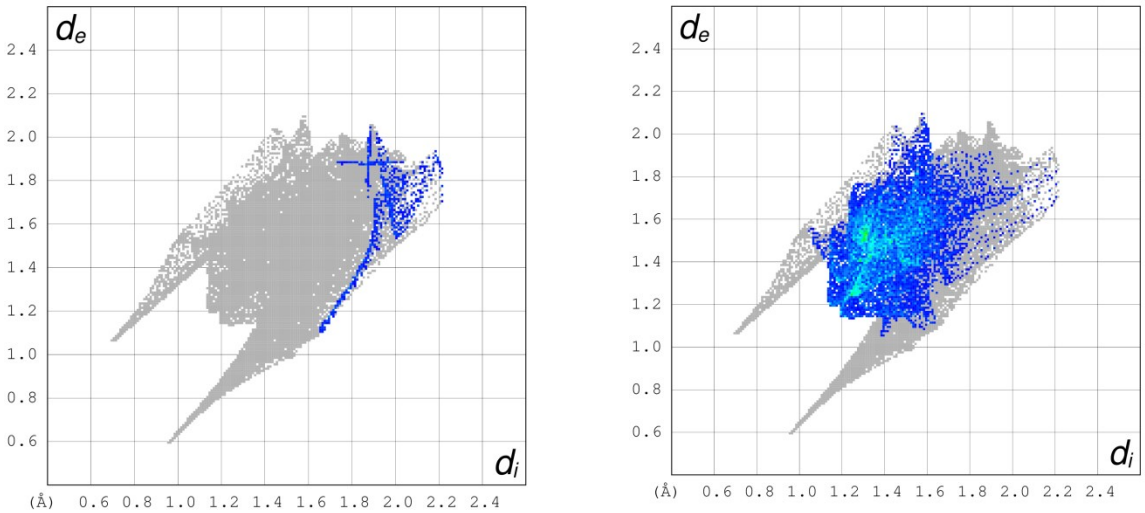

C···C **C···O**

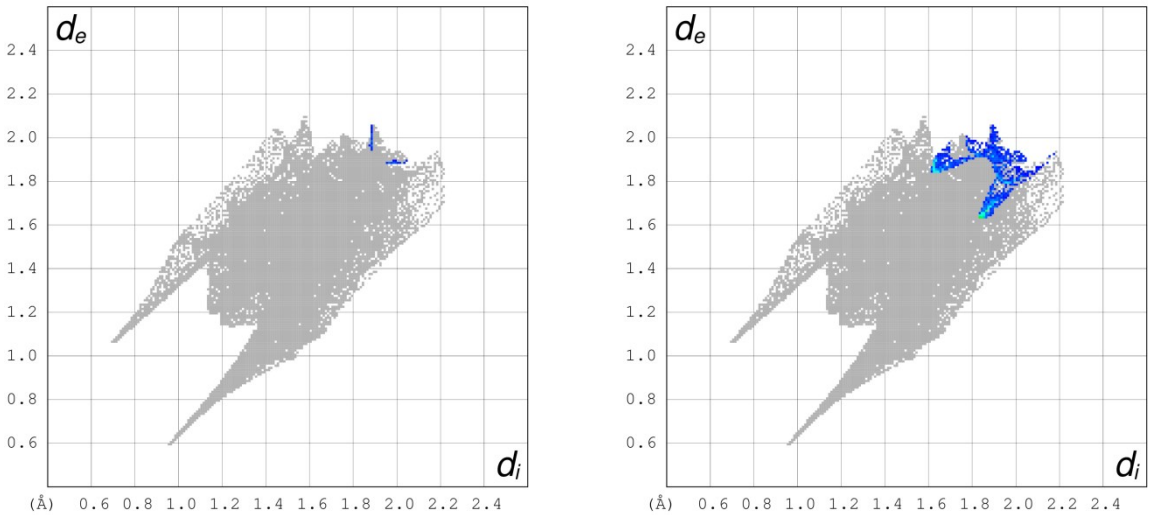

Figure S6. Decomposed fingerprint plots of GA-H molecule (compound **1**)

N···H

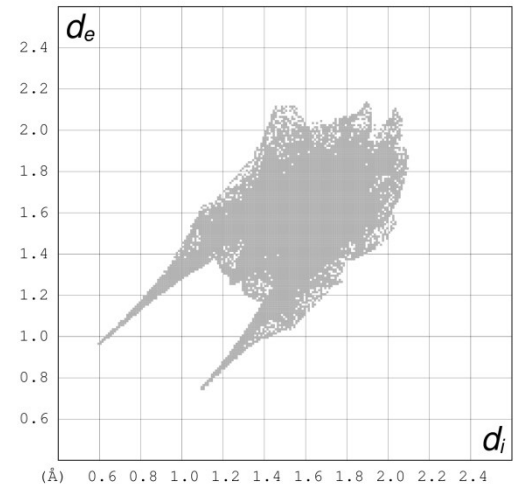

O···H

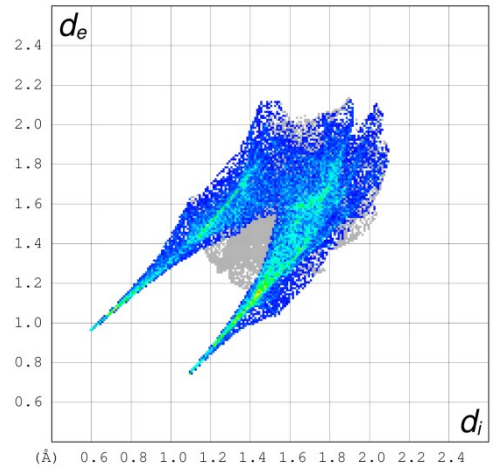

C···H

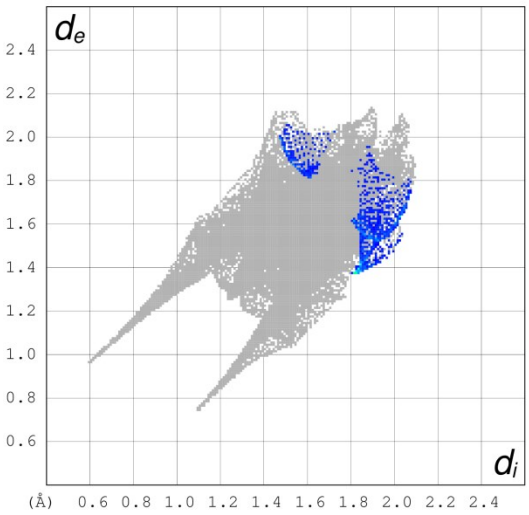

H···H

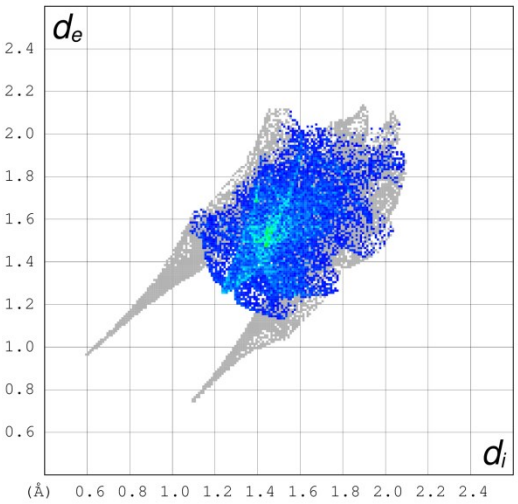

C···C

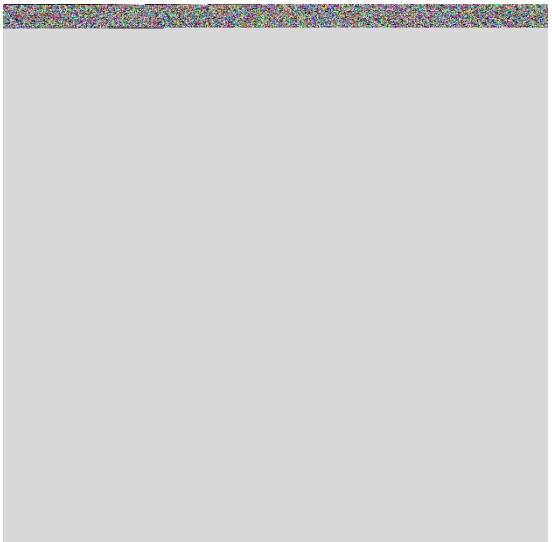

C···O

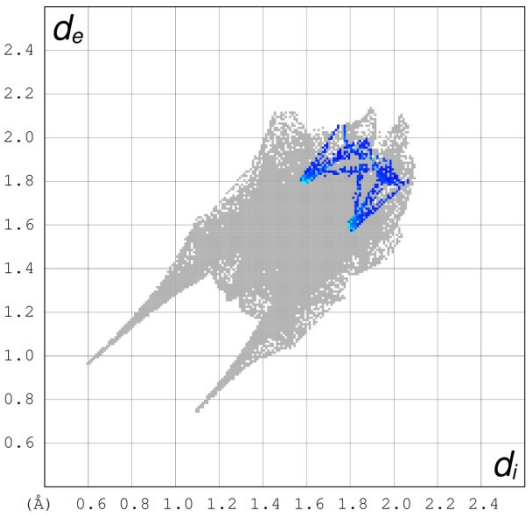

Figure S7. Decomposed fingerprint plots of GA molecule (compound **1)**

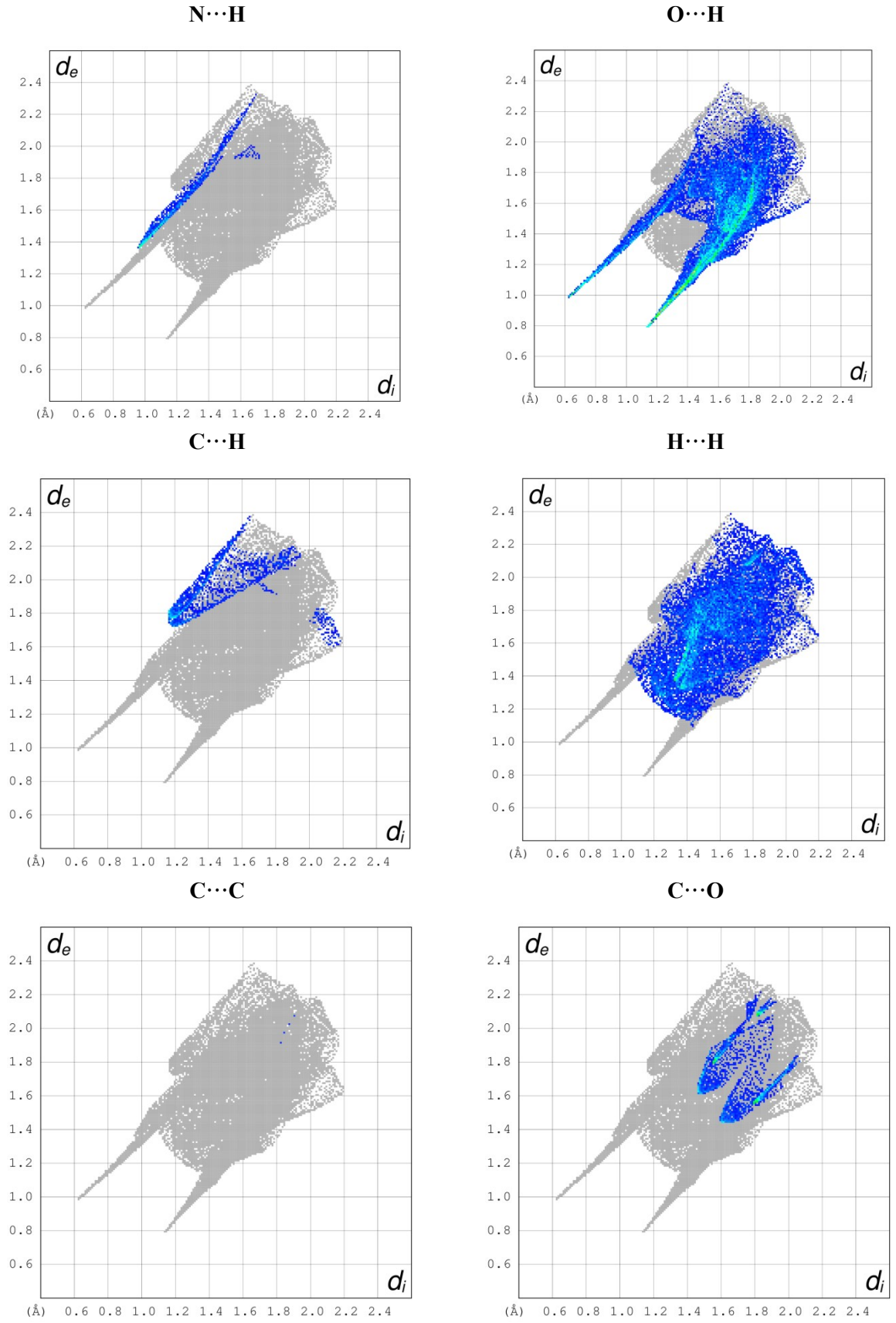

Figure S8. Decomposed fingerprint plots of GA molecule (compound **2)**

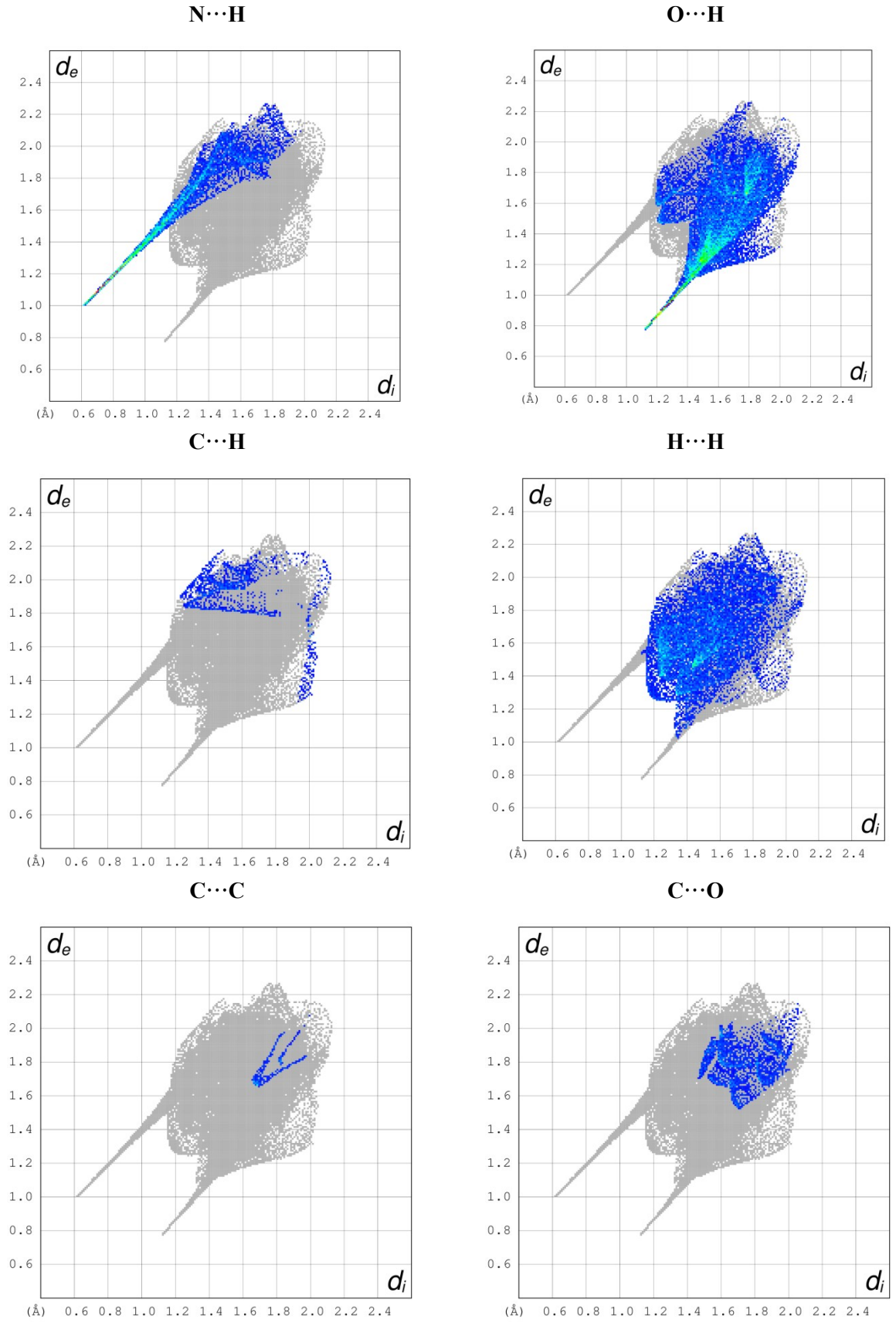

Figure S9. Decomposed fingerprint plots of GA molecule (compound **3)**

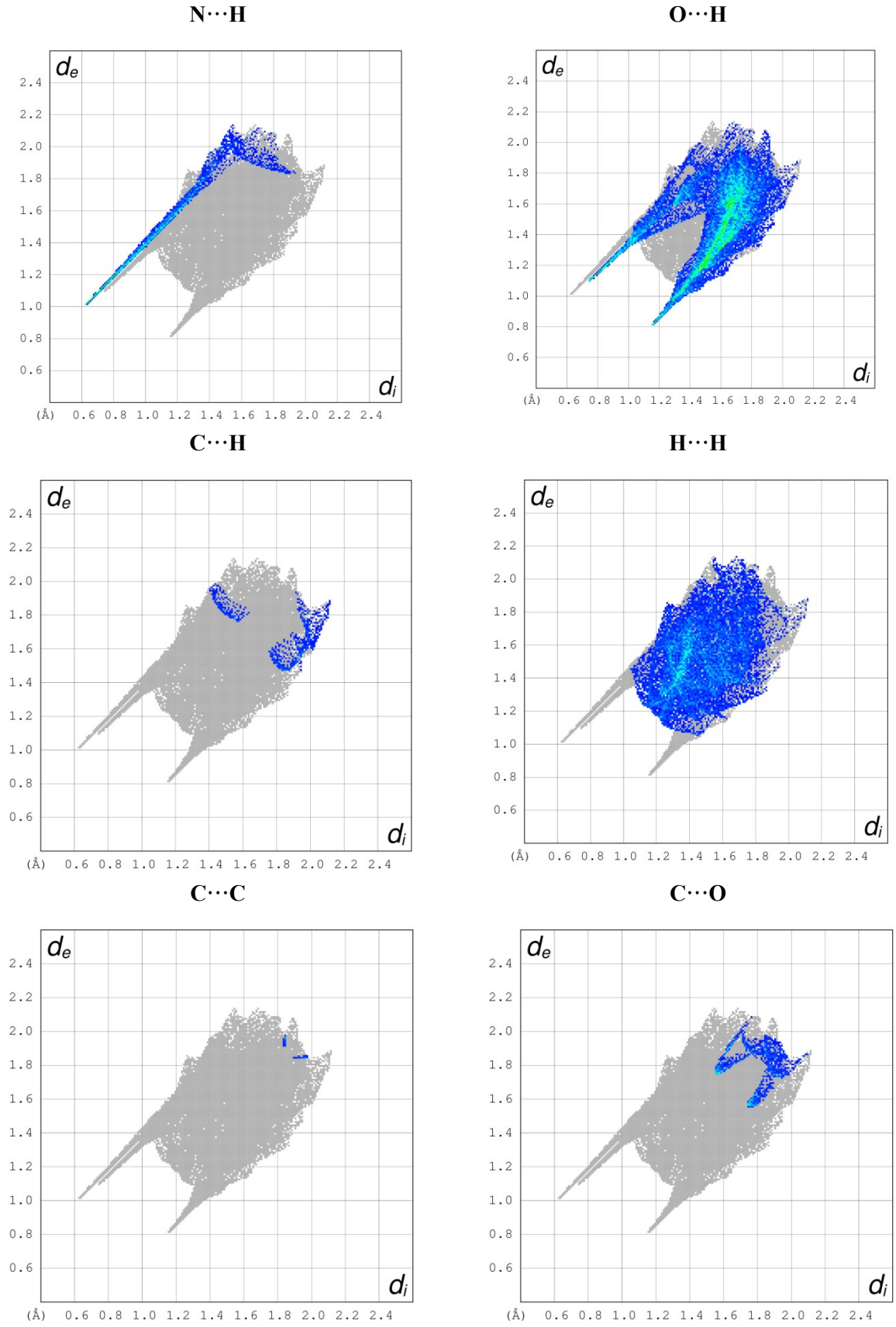

Figure S10. Decomposed fingerprint plots of GA molecule (compound **4)**

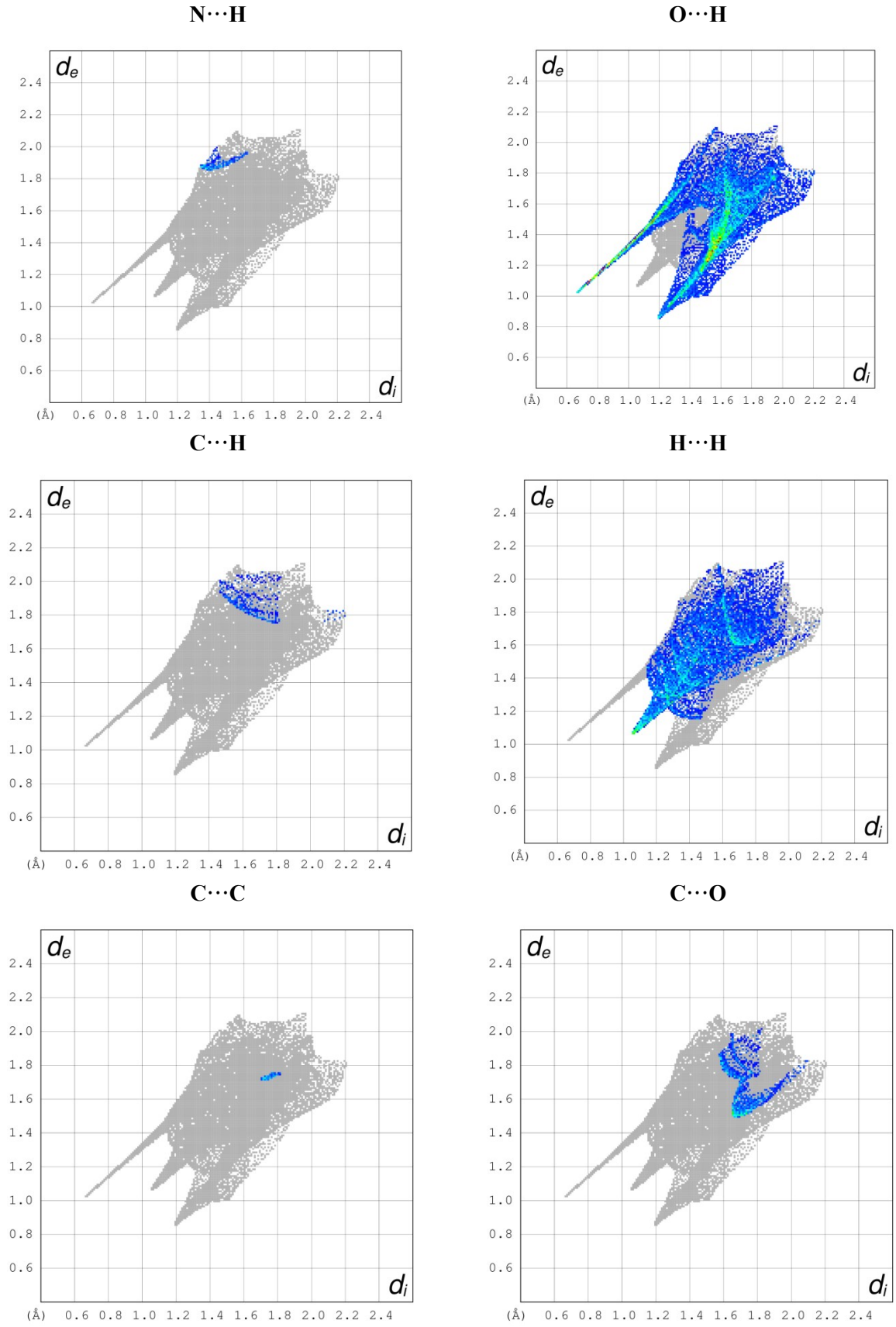

Figure S11. Decomposed fingerprint plots of GA molecule A (**5A**)

N···H **O···H**

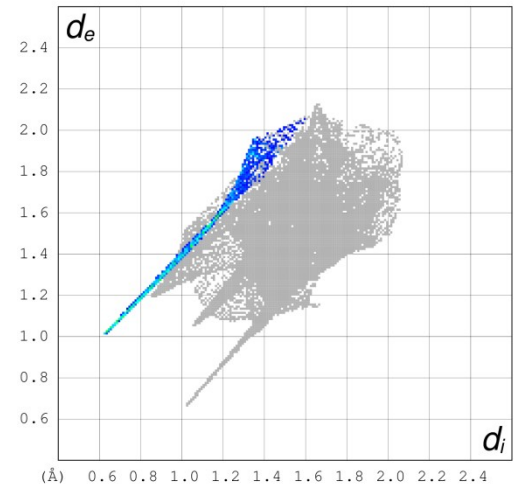

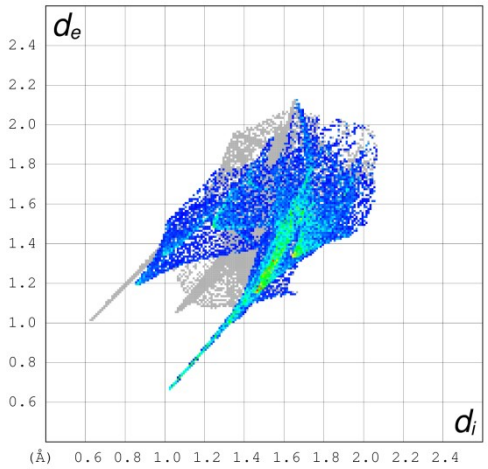

C···H **H···H**

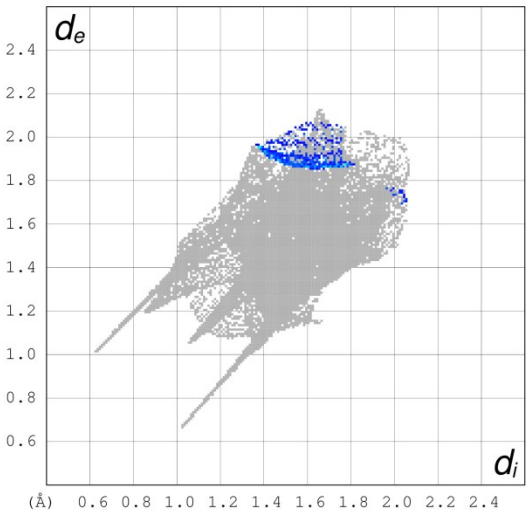

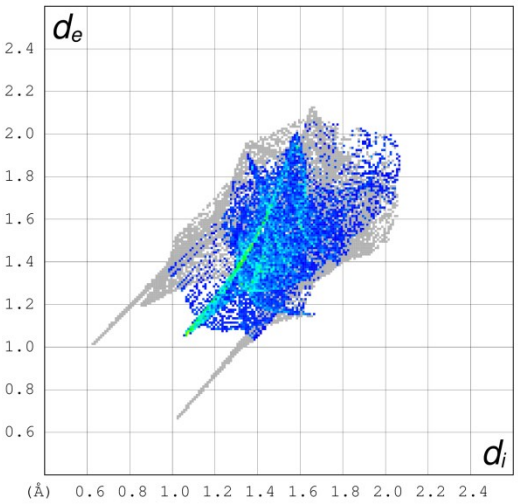

C···C **C···O**

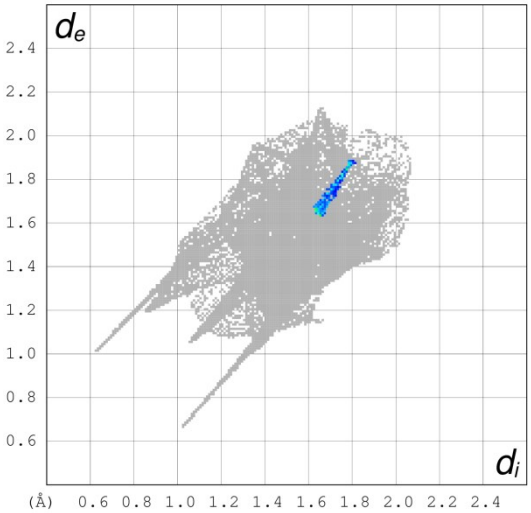

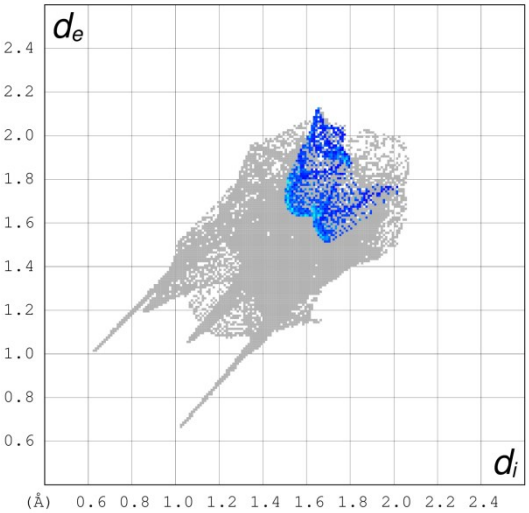

Figure S12. Decomposed fingerprint plots of GA molecule B (**5B**)

Comparison of HS properties of 1 with those of pure acid (CSD Refcode GLICAC01)

As we noted in crystal structure description section, the supramolecular network of **1** shares significant similarities with the hydrogen-bonding architecture of the glycolic acid itself (CSD Refcode GLICAC01) [6], given that NH_4^+ component features low molecular volume and high hydrogen-bonding capability. Accordingly, we compared their HS properties in terms of percentage shares of contact contributions (Table S3). One sees that the percentage shares for each of two crystallographically independent GA molecules of glycolic acid contribute to about 66% of all contacts, which is only four percentage points higher than for GA in ionic co-crystal **1** (**1B**). Substantial difference is identified in O···O contacts, which are almost not present in **1A** and **1B** (1.7% and 1.6%, respectively), but which are found in glycolic acid crystal structure (2.9% and 5.4%). Low share of O···O contacts in **1** we ascribe to the shielding effect of NH_4^+ cation as a result of an extensive formation of HBs with oxygen donors, which in turn effectively precluded GA and GA-H molecules from short contacts of this type.

Table S3. Contributions to the HS of crystallographically independent GA molecules (denoted as A and B) in the crystal structure of glycolic acid (CSD Refcode GLICA01).

Comp/CSD ref.		O···H/H···O	H···H	C···H/H···C	C···C	N···H/H···N	C···/O···C	N···C/C···N	O···O
GLICAC01, mol. A	GA	66.7	26.5	2.5	0	N/A	1.5	N/A	2.9
GLICAC01, mol. B	GA	65.2	24.5	2.1	0	N/A	3	N/A	5.4

References

1. N. Schultheiss and A. Newman, *Cryst. Growth Des.,* 2009, **9**, 2950-2967.
2. G. Socrates, Infrared Characteristic Group Frequencies, 2nd ed., John Willey & Sons, Chischester, England, 1994.
3. C. B. Aakeröy, A. Rajbanshi, Z. Jane Li and J. Desper, *CrystEngComm*., 2010, **12**, 4231–4239.
4. V. Mohaček-Grošev, V Šoštarić, A. Maksimovic, *Spectrochim. Acta A*, 2015, **140**, 35–43.
5. M. K. Stanton and A. Bak, *Cryst. Growth Des*., 2008, **8**, 3856-3862.
6. W. P. Pijper, *Acta Crystallogr.*, 1971, **B27**, 344-348.